

# Free-Standing, Patternable Nanoparticle/Polymer Monolayer Arrays Formed by Evaporation Induced Self-Assembly at a Fluid Interface

Jiebin Pang,<sup>†</sup> Shisheng Xiong,<sup>†</sup> Felix Jaeckel,<sup>§</sup> Zaicheng Sun,<sup>†</sup> Darren Dunphy,<sup>†</sup> and C. Jeffrey Brinker<sup>\*,†,‡</sup>

*NSF/UNM Center for Micro-Engineered Materials, Department of Chemical and Nuclear Engineering, The University of New Mexico, Albuquerque, New Mexico 87131, Advanced Materials Lab, Sandia National Laboratories, 1001 University Blvd SE, Albuquerque, New Mexico 87106, and Center for High Technology Materials, The University of New Mexico, Albuquerque, New Mexico 87106*

Received December 14, 2007; E-mail: cjbrink@sandia.gov

Ordered nanoparticle (NP) monolayers are of fundamental interest as 2D artificial solids in which electronic, magnetic, and optical properties can be tuned through electron charging and quantum confinement of individual NPs mediated by coupling interactions with neighboring NPs.<sup>1,2</sup> They are also of technological interest for a diverse range of applications including photovoltaics,<sup>3</sup> sensors,<sup>4</sup> catalysis,<sup>5</sup> and magnetic storage.<sup>6</sup> To date a myriad of techniques including Langmuir–Blodgett (LB) deposition,<sup>1,7,8</sup> droplet evaporation,<sup>9–12</sup> and interfacial assembly<sup>13</sup> have been used to organize monosized, hydrophobic NPs into ordered 2D arrays. It is generally agreed that for all these approaches NP assembly is driven by attractive van der Waals interactions balanced by steric repulsion.<sup>14</sup> However, under attractive conditions, depending on the competing effects of NP diffusion, convection, and solvent dewetting, a variety of patterns can emerge including ordered 2D and 3D arrays as well as fractal aggregates, ‘coffee rings’, and percolation clusters.<sup>15–18</sup> For this reason maintaining NPs at a fluid interface—either in evaporating droplets<sup>13</sup> or at a water surface<sup>19</sup>—has been successful in creating rather large scale, ordered NP monolayers. van der Waals interactions confined to NP interstices confer to these monolayers a high Young’s modulus allowing them to be prepared as free-standing membranes spanning 500-nm apertures<sup>13</sup> and to be transferred from a water surface to a solid substrate via microcontact printing using a prepatterned poly-(dimethylsiloxane) (PDMS) stamp.<sup>19,20</sup>

Here we extend the burgeoning work on NP monolayer fabrication in three substantive respects. First, we assemble hydrophobic gold NPs on a water interface from toluene containing polymethylmethacrylate (PMMA). In this case solvent evaporation concentrates the thinning film in NPs and PMMA, leading to NP self-assembly and solidification into an ordered NP/polymer nanocomposite monolayer with physical dimensions of up to 10 cm<sup>2</sup> (see Figure 1a). Second, the NP/PMMA monolayer can be transferred to arbitrary substrates and remains stable as a free-standing membrane suspended over cm-sized holes—even with free edges (Figure 1a). Third, the PMMA serves as a photoresist enabling two modes of electron beam (e-beam) NP patterning. Lower e-beam doses direct differential NP solubility and result in NP patterns with somewhat diffuse interfaces as shown previously for e-beam patterning of 1-dodecanethiol ligated Au monolayers deposited on silicon nitride<sup>21</sup> (Figure 2a,b). At higher e-beam doses the PMMA serves as a negative resist resulting in submicrometer patterns with edge roughness comparable to that of the NP diameter (Figure 2c,d). In combination these extensions contribute to the ability to integrate

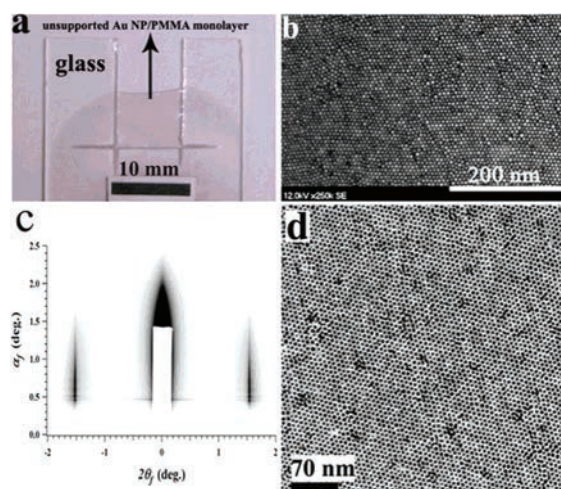


**Figure 1.** (a) Optical image of NP/PMMA film transferred to glass, arrow shows ~1 cm<sup>2</sup> unsupported area; (b) SEM image of NP/PMMA film transferred to silicon; (c) GISAXS pattern of film prepared as in (b); and (d) TEM of free-standing NP/PMMA film on a holey carbon grid.

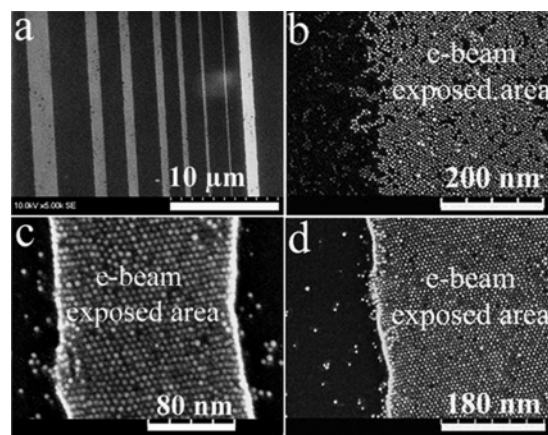


**Figure 2.** SEM images of ultrathin Au NP/PMMA films patterned with electron beam lithography. (a,b) Film patterned with lower e-beam dose and developed with hexane. (c, d) Film patterned with higher e-beam dose and developed with toluene plus 1-dodecane thiol (10:1 in volume).

NP arrays into robust micro- and macroscale devices. Additionally this approach represents a new means to attain very highly loaded yet flexible particle/polymer nanocomposites,<sup>18</sup> which have eluded most synthetic efforts to date.

Monosized, 1-dodecanethiol-ligated Au nanoparticles (about 5.5 nm in diameter) were synthesized by a modified single-phase method<sup>22</sup> (see the Supporting Information). For monolayer self-

<sup>†</sup> Department of Chemical and Nuclear Engineering, The University of New Mexico.

<sup>‡</sup> Sandia National Laboratories.

<sup>§</sup> Center for High Technology Materials, The University of New Mexico.

assembly, 60 mg of nanoparticles were dissolved in 6 mL of toluene containing 100 mg of PMMA ( $M_w = 996\,000$ , Aldrich). To prepare the NP/polymer monolayer, one drop (about 2–3  $\mu\text{L}$ ) of the NP/PMMA/toluene solution was carefully dispensed onto the surface of deionized water contained in an uncovered beaker. The droplet quickly spread onto the water surface (within  $\sim 1$  s) forming an approximately 50- $\mu\text{m}$  thick film with area of  $\sim 5$  cm. Evaporation-driven polymer solidification of the film perimeter establishes the maximum extent of spreading and pins the three-phase liquid/solid/vapor interface. Further evaporation necessarily thins the film maintained at constant area (at the very last stage of drying a slight radial contraction is observed). Based on the progression of optical interference fringes, we know that the film thins from the perimeter and imagine that, correspondingly, NP self-assembly and solidification proceed in a radially directed manner. If, as recently shown for hydrophobic Au NPs assembled within an evaporating droplet of toluene on a solid support,<sup>12</sup> NPs are captured and preferentially localized at the liquid/vapor interface, nucleation and growth of ordered NP array islands could proceed to a large extent within this fluid interface before evaporation-driven polymer solidification, explaining the formation and stabilization of the large area NP arrays we observe.

NP/polymer monolayer films were transferred to solid and porous substrates by lowering the substrate through the water surface, contacting the film edge, and vertical withdrawal. As shown in Figure 1a, large areas of homogeneous, supported and free-standing films can be formed in this manner. Profilometry indicated the film to be about 50-nm thick.

Physical properties of the Au NP/PMMA monolayer were characterized by standard electron microscopy and UV–visible spectroscopy along with grazing incidence small-angle X-ray scattering (GISAXS). Figure 1b,d shows representative SEM and TEM images of solid-supported and free-standing NP/PMMA monolayers, respectively. Ordering is commensurate with that observed previously for pure organic-ligated NP arrays formed on solid or fluid surfaces.<sup>19,22</sup> However comparison of center-to-center NP spacings of monolayer arrays assembled without and with PMMA shows a reduction from 7.5-nm (TEM not shown) to 6.3-nm (analysis of the GISAXS data, Figure 1c), respectively. This contraction is perhaps unexpected in consideration of the added PMMA. Conceivably the PMMA is at both interfaces, and its evaporation-driven solidification serves to compress slightly the monolayer at the final stage of drying. The GISAXS pattern in Figure 1c shows exclusively vertically modulated diffraction lines (as opposed to spots associated with 3D superlattices) consistent with long-range, in plane order expected for a 2D monolayer. UV–visible spectroscopy of the Au NPs in bulk toluene versus self-assembled in a PMMA composite monolayer show an approximate 40–50 nm ( $\sim 0.2$  eV) shift of the plasmon resonance frequency to lower energy (see the Supporting Information). Based on a classical model of the plasma frequency, this shift can be interpreted as arising from the higher dielectric constant of the medium surrounding an individual NP due to its six in plane NP neighbors.<sup>1</sup>

For many anticipated uses, it is desirable to pattern the NP arrays in arbitrary shapes, spanning a range of length scales. PMMA can be used as either a positive or a negative e-beam photoresist. Here we demonstrate two types of negative mode patterning (e-beam exposed regions are preserved). NP/PMMA monolayers supported on Si (100) wafers or glass slides were patterned using a JEOL 848 SEM (40 keV acceleration voltage) with NPGS lithography

software. Two exposure dose ranges were investigated. For the range 300–3000  $\mu\text{C}/\text{cm}^2$ , we find that NPs in the exposed regions are insoluble in hexane (5 min immersion) relative to the unexposed regions (Figure 2a,b). Presumably this dose strips the dodecane-thiol groups as reported for Au NPs assembled on solid supports<sup>21</sup>—the interface in this case is somewhat diffuse, and some Au NPs are dissolved from PMMA in the exposed areas (PMMA remains in both areas). For doses ranging from 10 000 to 30 000  $\mu\text{C}/\text{cm}^2$ , PMMA is cross-linked to become toluene insoluble,<sup>23</sup> serving as a negative resist when developed in toluene (Figure 2c,d). In this case the edge roughness is reduced to about the NP diameter, and the Au NPs are largely retained in the exposed areas.

We report a general and facile method to prepare free-standing, patternable NP/polymer monolayer arrays by interfacial NP assembly within a polymeric photoresist. The ultrathin monolayer nanoparticle/polymer arrays are transferable to arbitrary substrates and patternable by e-beam lithography, needed for applications in photovoltaics, sensors, catalysis, and magnetic storage. This approach to robust NP/polymer monolayers can be extended to other hydrophobic semiconductor and magnetic nanoparticles such as CdSe and FePt.

**Acknowledgment.** This work is supported by the DOE Office of Basic Energy Sciences, AFOSR, and ARO. Use of the Advanced Photon Source was supported by the DOE Office of Basic Energy Sciences under Contract No. DE-AC02-06CH11357.

**Supporting Information Available:** Synthesis of Au NPs, visible absorption spectra of Au NP and monolayer, and TEM image of CdSe NP monolayer. This material is available free of charge via the Internet at <http://pubs.acs.org>.

## References

- (1) Heath, J. R.; Knobler, C. M.; Leff, D. V. *J. Phys. Chem. B* **1997**, *101*, 189–197.
- (2) Pileni, M. P. *Appl. Surf. Sci.* **2001**, *171*, 1–14.
- (3) Oregan, B.; Gratzel, M. *Nature* **1991**, *353*, 737–740.
- (4) Jiang, C. Y.; Markutsya, S.; Pikus, Y.; Tsukruk, V. V. *Nat. Mater.* **2004**, *3*, 721–728.
- (5) Haruta, M. *Gold Bull. (London)* **2004**, *37*, 27–36.
- (6) Sun, S. H.; Murray, C. B.; Weller, D.; Folks, L.; Moser, A. *Science* **2000**, *287*, 1989–1992.
- (7) Kim, F.; Kwan, S.; Akana, J.; Yang, P. D. *J. Am. Chem. Soc.* **2001**, *123*, 4360–4361.
- (8) Schultz, D. G.; Lin, X. M.; Li, D. X.; Gebhardt, J.; Meron, M.; Viccaro, P. J.; Lin, B. H. *J. Phys. Chem. B* **2006**, *110*, 24522–24529.
- (9) Motte, L.; Billoudet, F.; Lacaze, E.; Douin, J.; Pileni, M. P. *J. Phys. Chem. B* **1997**, *101*, 138–144.
- (10) Rabani, E.; Reichman, D. R.; Geissler, P. L.; Brus, L. E. *Nature* **2003**, *426*, 271–274.
- (11) Tang, J.; Ge, G. L.; Brus, L. E. *J. Phys. Chem. B* **2002**, *106*, 5653–5658.
- (12) Bigioni, T. P.; Lin, X. M.; Nguyen, T. T.; Corwin, E. I.; Witten, T. A.; Jaeger, H. M. *Nat. Mater.* **2006**, *5*, 265–270.
- (13) Mueggenburg, K. E.; Lin, X. M.; Goldsmith, R. H.; Jaeger, H. M. *Nat. Mater.* **2007**, *6*, 656–660.
- (14) Narayanan, S.; Wang, J.; Lin, X. M. *Phys. Rev. Lett.* **2004**, *93*, 135503.
- (15) Redl, F. X.; Cho, K. S.; Murray, C. B.; O'Brien, S. *Nature* **2003**, *423*, 968–971.
- (16) Shevchenko, E. V.; Talapin, D. V.; Kotov, N. A.; O'Brien, S.; Murray, C. B. *Nature* **2006**, *439*, 55–59.
- (17) Deegan, R. D.; Bakajin, O.; Dupont, T. F.; Huber, G.; Nagel, S. R.; Witten, T. A. *Nature* **1997**, *389*, 827–829.
- (18) Shenhar, R.; Norsten, T. B.; Rotello, V. M. *Adv. Mater.* **2005**, *17*, 657–669.
- (19) Santhanam, V.; Liu, J.; Agarwal, R.; Andres, R. P. *Langmuir* **2003**, *19*, 7881–7887.
- (20) Santhanam, V.; Andres, R. P. *Nano Lett.* **2004**, *4*, 41–44.
- (21) Lin, X. M.; Parthasarathy, R.; Jaeger, H. M. *Appl. Phys. Lett.* **2001**, *78*, 1915–1917.
- (22) Lin, X. M.; Jaeger, H. M.; Sorensen, C. M.; Klabunde, K. J. *J. Phys. Chem. B* **2001**, *105*, 3353–3357.
- (23) Hoole, A. C. F.; Welland, M. E.; Broers, A. N. *Semicond. Sci. Technol.* **1997**, *12*, 1166–1170.

JA710994M